

Application of the arbitrary Lagrangian-Eulerian method to simulate electrical coalescence and its experimental verification

Grigorii Utiugov, Vladimir Chirkov*, Marina Reznikova

St. Petersburg State University, 7/9 Universitetskaya nab., St. Petersburg, 199034, Russia

* Corresponding author: v.chirkov@spbu.ru (Vladimir Chirkov)

Received: 16 March 2021

Revised: 25 June 2021

Accepted: 22 July 2021

Published online: 27 July 2021

Abstract

Under the action of a strong electric field, conducting droplets suspended in a dielectric liquid deform, attract each other, and can merge after their touching. The latter processes are called electrodeformation and electrocoalescence. The arbitrary Lagrangian-Eulerian method is one of the available approaches to simulate two-phase media, which has one crucial advantage over other techniques: it lets describing step-change in liquid properties when crossing the interface between two fluids. However, it generally fails to simulate volume merging or separation (i.e., changing topology). Suggested here is a computational model, where the idea of how-to-describe topology change during electrocoalescence is implemented. The model was developed for one of the most complex problems when electrical conductivities of contacting phases differ by many orders of magnitude. Numerical results were experimentally verified, which enables the model application to describe electrohydrodynamic processes in two-phase immiscible liquids and, in particular, electrocoalescence.

Keywords: Electrocoalescence, electrohydrodynamics, moving mesh, two-phase liquid, water-oil emulsion.

1. Introduction

Electrocoalescence is a merger process of two (or more) volumes of a conductive liquid under the action of an electric field [1]. These volumes may be droplets of one liquid suspended in a non-conductive medium or, e.g., droplets placed on a dielectric substrate. On one hand, the corresponding investigation is a topical task since droplets combining under the action of an electric field underlies electrocleaning technology of liquids from the tiniest droplets of water [2–5], as well as other technologies [6, 7]. On the other hand, this process's numerical simulation is still quite a complicated task since it includes solving non-linear electrohydrodynamic equations and describing phase distribution. The latter is a non-trivial problem, especially when a considerable difference in properties of contacting phases (e.g., when conducting droplets is suspended in a liquid dielectric) [8, 9].

Many numerical models of electrical electrohydrodynamic processes in two-phase liquids where the reliability of numerical results is questionable can be found in the literature (e.g., [4, 10, 11]). For example, these unjustified results can be expressed in the non-equipotentiality of conducting media volume [4, 10] or the space charge "escape" from the interface location [11]. The related issues are discussed in [12], where a modification of the phase-field method [13–15] is proposed. Despite this recent success in applying the technique for the simulation of droplet electrodeformation, there is still an issue about correct values of parameters introduced in the phase-field theory—the interface thickness and the mobility tuning parameter—that do not have direct counterparts in classical fluid dynamics [15]. In turn, there are few papers where the above-mentioned problems seem to be avoided when simulating electrical coalescence [16–18]. Paper [16] uses the boundary integral method and yields quite close results to the experimental data; however, a simplification in the Navier-Stokes equation is made (namely, the Stokes flow regime is considered). Two other papers [17, 18] employ a coupled level-set and volume-of-fluid method [19]. The latter technique requires interface

reconstruction for every time step [20] and leads to an unsmooth distribution of space charge density, and the authors computed tasks under highly viscous conditions. Nevertheless, all these models can be used for numerical simulation of electrocoalescence.

Proposed below is an alternative to the above approaches. Computing the threshold between electrical coalescence and non-coalescence is an important task in designing electrocoalescers. Estimating the corresponding values lets one choose voltage magnitude to increase the device performance. However, solving the issue calls for many computations that include the droplet approaching stage, the emergence of a bridge, and resulting coalescence or non-coalescence. The accuracy of the model used, as well as its computational cost, is of paramount importance. The model based on the arbitrary Lagrangian-Eulerian approach or the so-called moving mesh method [21] has no diffuse interface and no drawbacks of the phase function model and shows comparably low resource intensity. The numerical technique enables describing two-phase media when the electrical conductivities of two contacting media differ significantly. The boundary between phases is represented by a line of geometry that moves according to the fluid velocity's calculated value throughout the entire solution. Still, this method disallows considering the process of the object's topology changing, particularly droplets combining, and is applied usually to simulate deformation or movement of droplets [22–24].

However, the latter hindrance can be overcome using the following idea. The analysis of the experimental data on electrocoalescence [25–28] has shown that the changing object's topology—the creation of a bridge between the droplets—happens so swiftly (less than 0.1 ms) that the geometry of the droplets almost does not change during the corresponding time span (Fig. 1). According to this, one may conduct the simulation of electrical coagulation by stopping the calculation immediately before droplet touching (at a finite distance that can be chosen in advance), introducing a bridge between droplets to the numerical model, and resuming the computation. The present work investigates the possibility of applying the approach to simulate the electrical coalescence of droplets and estimate the threshold electric field strength between coalescence and non-coalescence.

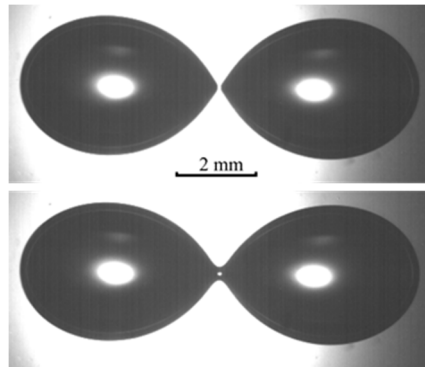


Fig. 1. Water droplet photos before and after the formation of the water bridge between them; the outer liquid is olive oil, droplet radii 1.97 mm, temperature +22 °C, voltage 4.95 kV, the interelectrode gap is 3 cm (average electric field 1.65 kVcm⁻¹), the time between frames 1 ms.

2. Numerical model

2.1 Set of equations and boundary conditions

The arbitrary Lagrangian-Eulerian method is applied to simulate the electrical coalescence of two conductive droplets (distilled water) suspended in the dielectric phase (olive oil) and placed in the center of a cell with two flat parallel electrodes (Fig. 2a). The numerical model bases on the Navier-Stokes, continuity, and Poisson equations:

$$\rho \frac{\partial \vec{v}}{\partial t} + \rho(\vec{v}, \nabla)\vec{v} = -\nabla P + \nabla \cdot \eta(\nabla \vec{v} + \nabla \vec{v}^T) + \vec{f}_g \quad (1)$$

$$\operatorname{div}(\vec{v}) = 0 \quad (2)$$

$$\operatorname{div}(\varepsilon\varepsilon_0\vec{E}) = 0 \quad (3)$$

$$\vec{E} = -\nabla V. \quad (4)$$

Here \vec{E} is the electric field strength, V is the electric potential, \vec{v} is the fluid velocity, P is the pressure, ε is the relative electric permittivity, ε_0 is the vacuum permittivity, ρ is the mass density, η is the dynamic viscosity, t is the time, \vec{f}_g is the gravity force.

An interface displacement (i.e., finite-element mesh motion) is performed according to the fluid velocity calculated value. The Yeoh smoothing method [29] for mesh deformation is used in the numerical model:

$$W = \frac{1}{2} \int_{\Omega} c_1(I_1 - 3) + c_2(I_1 - 3)^2 + \kappa(J - 1)^2 d\tilde{V} \quad (5)$$

$$J = \det(\nabla_X x), I_1 = J^{-\frac{2}{3}} \operatorname{tr}((\nabla_X x)^T \nabla_X x). \quad (6)$$

Here W is the strain energy, I_1 and J are the invariants, \tilde{V} is the volume. Constant values are the following: $c_1 = 1$ (the artificial shear modulus), $c_2 = 100$ (the stiffening factor), κ is an artificial bulk modulus.

The droplet is believed to be a perfectly conducting one and its surface to be equipotential. Thus, the following simplification is made: the electrostatics equation is calculated for the dielectric liquid only, whereas hydrodynamic ones—for both phases. Besides, the gravity force is disregarded in the computations. Electrostatics and hydrodynamics subsets are interrelated via the electric force densities (pressures) P_C applied to the droplet surface [24]:

$$P_C = \frac{1}{2} \lambda E_n, \quad (7)$$

where λ is the surface charge density, E_n is the normal component of the electric field. The surface tension force P_{st} also acts on the droplet surface:

$$P_{st} = 2\gamma H, \quad (8)$$

where γ is the interfacial tension, H is the mean curvature of the interface. The following boundary condition is set at the boundary of the droplet to account for the forces densities mentioned above (pressures):

$$P_{in} - P_{out} = P_{st} - P_C, \quad (9)$$

where P_{in} and P_{out} are pressures near the interface inside and outside the droplet. The consistency of calculated hydrodynamic equations for both phases is realized through the equality of each phase velocity at the interface:

$$v_b = v_{oil} = v_{water}, \quad (10)$$

where v_b is the velocity of the boundary, v_{oil} and v_{water} are the velocities of the phases near the interface.

The numerical modeling uses COMSOL Multiphysics software based on the finite-element method. The geometry of the computer model and the boundary conditions are shown in Fig. 2b. The initial distance between the droplets was taken sufficiently large (at least $2R$) to let them deform completely and accelerate before touching each other; otherwise, the results are dependent on the corresponding distance. The following grid distribution was set in the model to provide computational accuracy of the results. Three hundred elements were built at the interface (which corresponds approximately to the element size $0.01R$), 100 elements—at the line between the droplet and the reflection symmetry plane. The maximum element size in the whole domain was 0.25 mm. The minimum element quality with the value of 0.3 was chosen as the condition for remeshing: when the ratio of the longest side of the element to the shortest one reached the specified value, the grid was rebuilt in the model. The assessment of whether the solution is grid-independent is presented in Section 3.2 basing on calculating the threshold between electrical coalescence and non-coalescence for different element sizes.

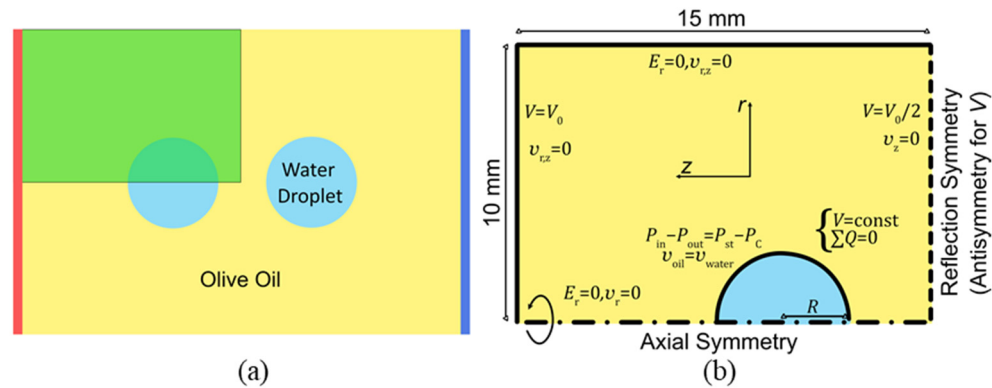


Fig. 2. (a) Schematic of the model geometry with the indication of the calculated area (highlighted with green color); (b) geometry and boundary conditions ($\sum Q$ is the total surface charge).

2.2 The key idea of the approach

As mentioned above, the direct computation of droplet coalescence is an infeasible task when using the arbitrary Lagrangian-Eulerian method due to the change of the object's topology during the process. However, the complete study can be divided into three subproblems. First, one needs to consider the droplets' deformation and their convergence under the electric field effect. The second step is to stop computation (when the distance between them goes below a predetermined value discussed below) and add a bridge between droplets (Fig. 3). The latter means changing the geometry and setting unified boundary conditions for the area of two droplets joined with the bridge. The proposed shape of the connection channel is a cylinder; its parameters are discussed in Section 3.2. Finally, the calculation has to be resumed using the first solution step's final result as the initial conditions. The computation of further dynamics of these droplets connected with the bridge enables getting the outcome of the process—the coalescence or non-coalescence. The former can be obtained if the surface tension force prevails over the Coulomb one; otherwise, the non-coalescence occurs (e.g., like is shown in Table 4).

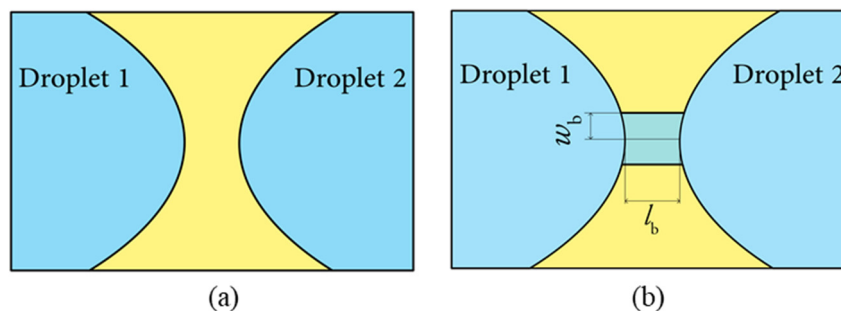


Fig. 3. Process of introducing the bridge: (a) droplet poles before adding the “bridge”, (b) droplet poles after adding the “bridge”.

A similar approach of stopping simulations before droplet contact and artificially creating a bridge was also suggested in a recent paper [30]. The authors use the boundary element method to investigate the effect of initial separation distance and electrocapillary number on the electrical coalescence. Unlike the present study, only the Stokes flow regime is considered in [30].

3. Results and discussion

The numerical simulation and experimental study were conducted for olive oil (as a dispersion medium) and distilled water (as dispersed phase) with the following properties: $\gamma = 16 \text{ mN m}^{-1}$, $\epsilon_{\text{oil}} = 2.85$, $\epsilon_{\text{water}} = 80$, $\rho_{\text{oil}} = 910 \text{ kg m}^{-3}$, $\rho_{\text{water}} = 998 \text{ kg m}^{-3}$, $\eta_{\text{oil}} = 65 \text{ mPa}\cdot\text{s}$, $\eta_{\text{water}} = 1 \text{ mPa}\cdot\text{s}$ [12]. The permittivity and interfacial tension were measured at the Research park of St. Petersburg State University. Further details on the experimental study can be found in [25, 31].

3.1 Solutions before and after adding the bridge

The first part of the results is devoted to demonstrating dependent variables' distributions during the electrical coalescence process, including times immediately before and after introducing the bridge into the model. Fig. 4 shows velocity and surface charge distributions for two droplets with $R = 1.97 \text{ mm}$ and voltage $V_0 = 4950 \text{ kV}$ (the average electric field strength 1.65 kV cm^{-1}); bridge parameters (according to Fig. 3b): $l_b = 0.01R$, $w_b = l_b$. The surface charge emerges at both droplets, then they deform and begin to move to each other after the voltage turn-on (Fig. 4a). The interaction between droplets is the dipole-dipole one. The sides of the droplets closest to each other sharpen, droplets stretch, and the surface charge density increases strongly on the sharpened edges before the moment of bridge formation (Fig. 4b). The velocity heightens as well and can reach several tens cm s^{-1} . It is worth noting that fluid motion and the corresponding kinetic energy are directly accounted for in computations. The higher the velocity of oncoming droplet movement, the easier the coalescence process.

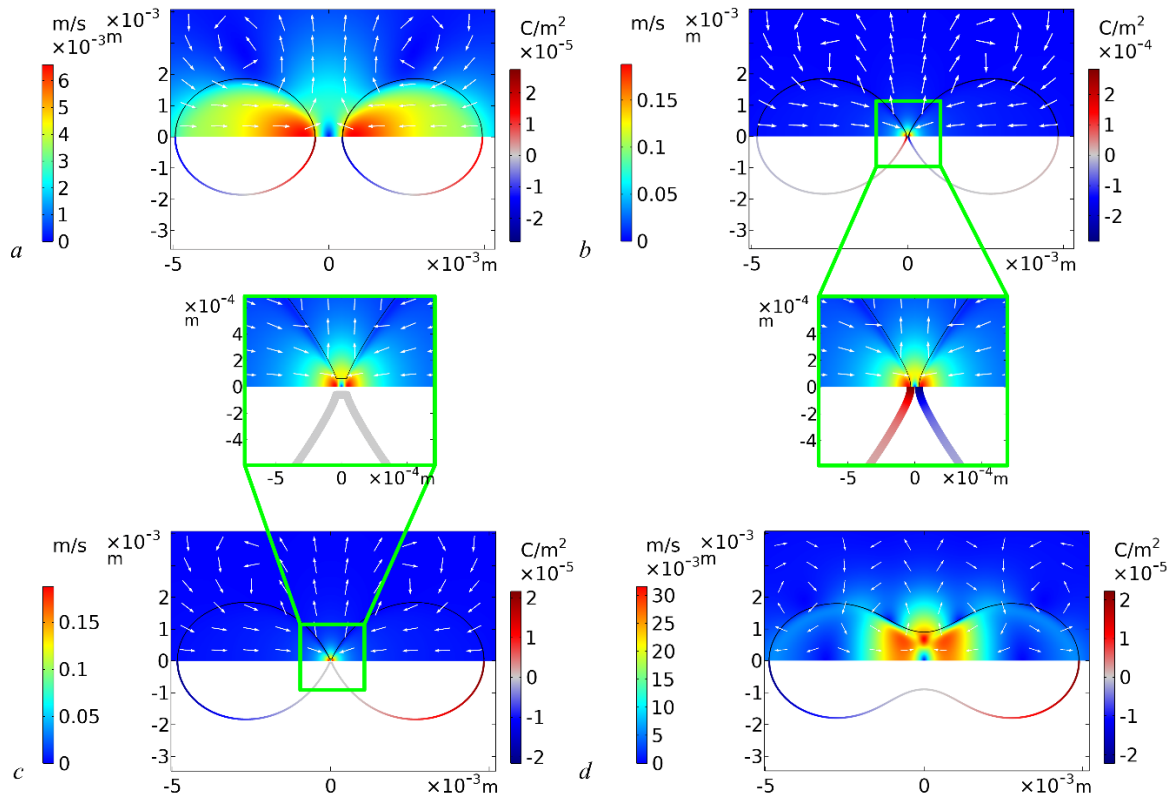


Fig. 4. Surface and arrow plots of the velocity distribution (the up part of every subfigure) and surface charge density distribution (the down part of every subfigure): (a) $t = -32 \text{ ms}$; (b) $t = 0 \text{ ms}$ before adding the bridge; (c) $t = 0 \text{ ms}$ after adding the bridge; (d) $t = 20 \text{ ms}$.

Immediately after the contact (Fig. 4c), the velocity distribution remains nearly the same; however, the surface charge redistributes: the bridge and adjoining parts of the consolidated droplet become neutral. After the bridge appears, it starts to thicken (Fig. 4d) (like it is described in [16]). The Coulomb force affects the water area and tries to break it into two droplets, whereas the surface tension force attempts to make the interface spherical. The outcome depends on the ratio between these two forces. In the considered case, the surface tension prevails, and the process yields electrical coalescence. On the contrary case, the bridge reduces in thickness and tries to break out. The obtained information is enough to conclude whether the process for the specified parameters yields coalescence or non-coalescence. However, one more geometry change is necessary if one needs to describe droplet separation (in the case of non-coalescence) and further process.

3.2 The effect of bridge parameters

The most non-evident part of the suggested method is introducing the bridge into the model. The corresponding parameters—initial radius and length of the bridge (Fig. 3)—have to be chosen in advance and substantiated. The length of the connection channel means to be its axial length. First of all, investigating the bridge parameters' effect on the study outcome is necessary to confirm the model's sustainability. One may suggest that the model allows getting the correct results if they are independent of the connection channel size below a certain level. The study is similar to the grid independence test—when the size of elements is small enough, the further their lessening has to yield quantitatively the same values of dependent variables.

In this model, the bridge's length can be chosen arbitrarily small since it is possible to simulate droplets' approach to any finite distance between them. The only reasonable restriction is to select the length value not too small to avoid a large number of geometry rebuildings and remeshings while droplets approach each other. According to the experimental data (Fig. 1), the connection channel length is about $0.01R$ at the moment of its appearance, whereas the ratio of the bridge length to its radius reaches approximately $1/1$ during 1 ms after the contact. The result obtained in the corresponding case is marked as "Ref. value" in Table 1. The channel length varied from ten times shorter to ten times larger than that observed in the experiment. The bridge radius was changed from four times shorter to four times larger value than the connection length. It is assumed that simulation results are the most precise ones that can be achieved in the numerical simulation when tiny bridges are used (e.g., when the bridge length to droplet radius ratio equals 0.001).

The effect of bridge parameters on the electric field strength threshold value (when the coalescence outcome of droplet interaction succeeds with the non-coalescence one) was investigated for droplet radius $R = 1.8$ mm. Though the model disallows getting the threshold value per se, a step-by-step increase in the voltage value enables the reversal of the numerical simulation outcome. The threshold was calculated as the average between two the closest voltages yielding coalescence and non-coalescence, whereas the error was estimated as half of the difference between the values. Computations were repeated many times for various bridge parameters.

The grid-independence test was made for reference values of bridge parameters: $l_b = 0.01R$, $w_b = l_b$. The size of elements was made two and four times worse (150 and 75 elements at the interface, 50 and 25 elements at the line between the droplet and the plane of the reflection symmetry, 0.5 mm and 1 mm—maximum domain element size correspondingly), and calculations of the threshold values were conducted. The variation in the threshold for the specified grid modification was not revealed, at least within the chosen step in the electric field strength change (17 V cm^{-1} , i.e., 0.4% of the threshold value).

The results on the threshold values for various bridge parameters are given in Table 1. Table 2 contains the relative change in the total water volume after adding the connection between droplets. It is worth noting that the axial height value cannot be specified precisely (it depends on the last saved computation time-step); therefore, Tables 1 and 2 describe the approximate values of bridge length ratio to the droplet radius. Nevertheless, the connection radius can be manually controlled, and the proportion between it and the connection length is strictly fulfilled.

Table 1. The dependence of the results on changes of bridge parameters.

l_b/R \ l_b/w_b	4/1	2/1	1/1	1/2	1/4
1/10	−100%	−4.0%	<0.4%	1.8%	8.9%
1/100	−2.2%	−1.3%	Ref. value	<0.4%	1.3%
1/1000	<0.4%	<0.4%	<0.4%	<0.4%	<0.4%

Table 2. The change of relative volume after adding the bridge (%).

l_b/R \ l_b/w_b	4/1	2/1	1/1	1/2	1/4
1/10	0.02	0.25	0.28	2.3	26.6
1/100	0.01×10^{-2}	0.01×10^{-2}	0.18×10^{-2}	0.61×10^{-2}	7.1×10^{-2}
1/1000	0.08×10^{-6}	0.3×10^{-6}	0.76×10^{-6}	2.3×10^{-6}	24×10^{-6}

The computed threshold electric field strength is $1.875 \pm 0.008 \text{ kV cm}^{-1}$ for the reference value of bridge parameters (Fig. 5a), leading to a 0.18% artificial increase in the relative volume of water after adding the connection channel (Table 2). The numerical model stability (within 0.4% to bridge changes) was confirmed for small connection channels with $l_b/R = 1/1000$ (the bottom line in Table 1) and those with its radius equals its length (the central row in Table 1). Using other bridges distorts the results and, in several cases, can be physically unreasonable (Fig. 5b and c). For instance, using $l_b/R = 1/10$ and $l_b/w_b = 1/4$ results in a thick bridge (Fig. 5c), which leads to a remarkable increase in the threshold since it simplifies droplet coalescence. In turn, using the same droplet radius/bridge length ratio and setting $l_b/w_b = 4/1$ (Fig. 5b) fails to get the threshold value—the bridge is too long and too thin to let droplets combine. Nevertheless, it is possible to receive correct results for $l_b/R = 1/10$ when the experimentally observed ratio between the channel length and width is used, although the water volume is artificially boosted by 0.3%. Thus, the obtained result depends on the bridge shape for large ratios between l_b and R (1/10 and 1/100), whereas they are independent of those for smaller ones.

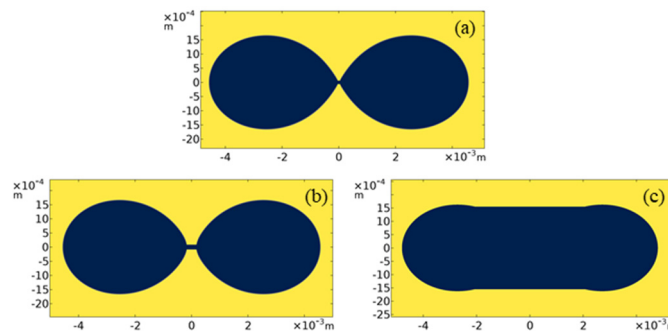


Fig. 5. Different types of the bridges (a— $l_b/R = 1/100$, $l_b/w_b = 1$; b— $l_b/R = 1/10$, $l_b/w_b = 4/1$; c— $l_b/R = 1/10$, $l_b/w_b = 1/4$).

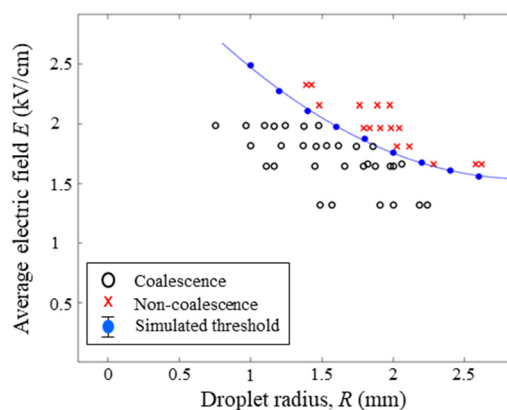


Fig. 6. The experimental statistical data on coalescence and non-coalescence (black circles and red crosses) and the simulated dependence of the threshold electric field value on the droplet radius.

3.3 Determination of the threshold between coalescence and non-coalescence

The outcome of the process—electrical coalescence or non-coalescence—depends on the voltage and the droplet radius. Thus, the suggested model can be verified with the experimental threshold voltage between

these two results (Fig. 6). The corresponding numerical simulation was carried out by changing the voltage for several droplet radii. For all computations, the bridge parameters were the following: $l_b = 0.01R$, $w_b = l_b$. Besides, the grid independence was checked for the droplet with maximum modeled radius $R = 2.6$ mm, which was done due to the deterioration of the grid quality for large droplets. The investigation was the same—the size of the elements was specified two and four times worse—and the threshold value remained the same.

The threshold between coalescence and non-coalescence was computed with the error ± 25 V (the average electric field strength ± 8 V cm⁻¹). The results obtained using the arbitrary Lagrangian-Eulerian method agree well with the experimental data. The approximating line for the computed threshold lies between the two areas corresponding to electrocoalescence and non-coalescence. It is worth noting that Fig. 6 covers only the macroscopic range since the latter was used for the proposed model verification. Nevertheless, the model can be used to study the electrical coalescence of micrometer-sized droplets, e.g., during the process of de-emulsification [1].

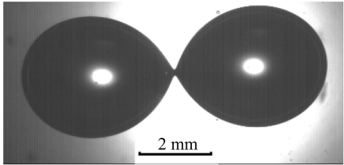
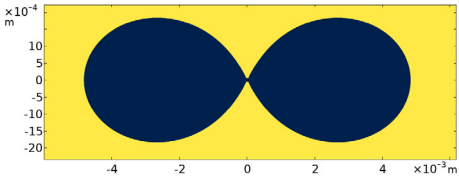
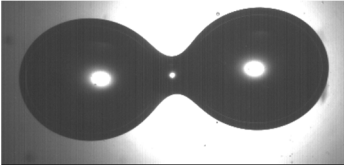
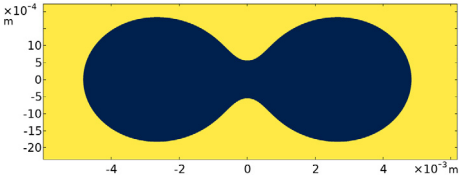
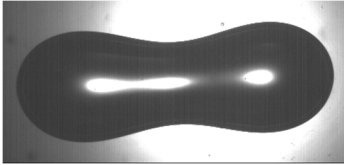
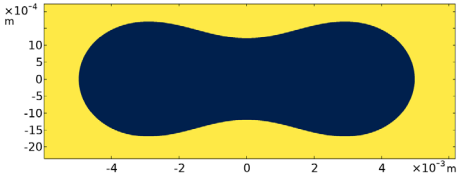
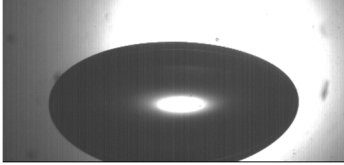
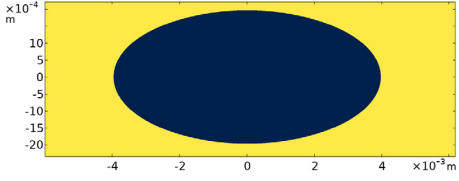
3.4 Comparison of the droplets dynamics with the experiment

Further on, the simulation of electrocoalescence and non-coalescence was conducted following available experimental data [25]:

- droplets with radius $R = 1.97 \pm 0.01$ mm, voltage $V = 4.95$ kV, the interelectrode distance 3 cm, $l_b = 0.01R$, $w_b = l_b$ for the electrocoalescence simulation;
- droplets with radius $R = 2.09 \pm 0.01$ mm, voltage $V = 5.95$ kV, the interelectrode distance 3 cm, $l_b = 0.01R$, $w_b = l_b$ for the non-coalescence simulation.

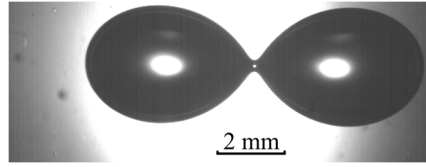
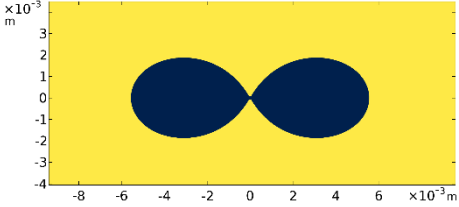
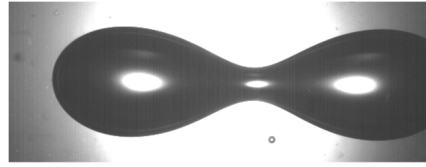
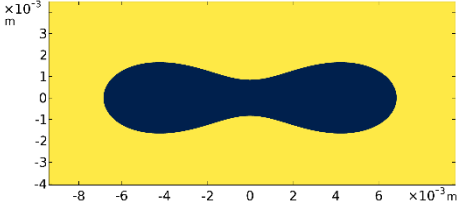
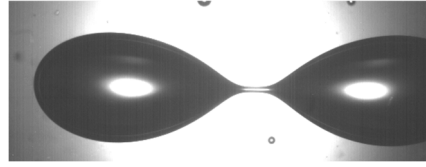
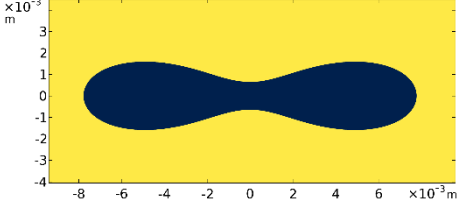
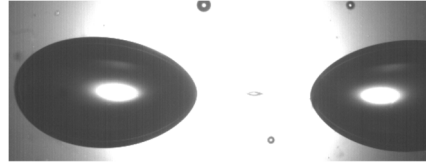
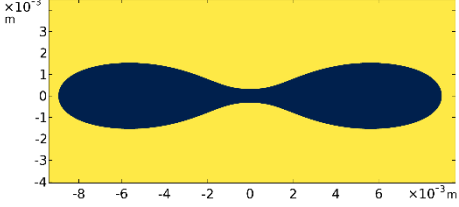
The comparison of the dynamic was conducted after the bridge introduction to the model and presented in Tables 3 and 4. In the case of electrocoalescence, a high level of accordance between droplet shapes, obtained in the experiment and the simulation, is observed throughout the whole transient process.

Table 3. Experimental video frames and modeling results of the electrocoalescence for droplets with radius $R = 1.97 \pm 0.01$ mm and applied voltage $V = 4.95$ kV.

Time (ms)	Experiment	Numerical simulation
0		
8.5		
35.5		
109		

For non-coalescence, there is some delay in droplets rupture in the simulation. The corresponding difference probably can be explained by the following. The interfacial tension value (at least for organic oils) is dependent on the contact time between two phases, according to data presented in [12, 32]. Consequently, the property can change during the coalescence process due to an increase in the interface area, providing new molecules of two immiscible liquids to get into contact [32]. At the same time, it is disregarded in the numerical model.

Table 4. Experimental video frames and modeling results of the non-coalescence for droplets with radius $R = 2.09 \pm 0.01$ mm and applied voltage $V = 5.95$ kV.

Time (ms)	Experiment	Simulation
0		
56		
77		
95		

4. Conclusion

The suggested approach does enable computing the electrocoalescence process using the arbitrary Lagrangian-Eulerian method. When parameters are correctly selected, the artificial introduction of the bridge between droplets does not distort the results and allows obtaining a good agreement in droplet dynamics during the transient process of electrical coalescence. The computed data on the threshold between coalescence and non-coalescence agree with the experimental data.

Acknowledgements

The study was supported by the Russian Science Foundation, research project No. 19-79-00127. The research was performed at the Research park of St. Petersburg State University “Computing Center,” “Center for Nanofabrication of Photoactive Materials (Nanophotonics),” “Center for Diagnostics of Functional Materials for Medicine, Pharmacology, and Nanoelectronics,” and “Center for Geo-Environmental Research and

Modeling (GEOMODEL).” The authors are grateful to a former student of St. Petersburg State University, Vitalii Yakovlev, who first proposed the idea of manual introducing the bridge during our discussions.

References

- [1] Atten P., Electrohydrodynamics of dispersed drops of conducting liquid: From drops deformation and interaction to emulsion evolution, *Int. J. Plasma Environ. Sci. Technol.*, Vol. 7 (1), pp. 2–12, 2013.
- [2] Eow J. and Ghadiri M., Electrostatic enhancement of coalescence of water droplets in oil: a review of the technology, *Chem. Eng. J.*, Vol. 85 (2–3), pp. 357–368, 2002.
- [3] Gong H., Li W., Zhang X., Peng Y., Yu B., and Mou Y., Simulation of the coalescence and breakup of water-in-oil emulsion in a separation device strengthened by coupling electric and swirling centrifugal fields, *Sep. Purif. Technol.*, Vol. 238, p. 116397, 2020.
- [4] Hadidi H., Kamali R., and Manshadi M.K.D., Numerical simulation of a novel non-uniform electric field design to enhance the electrocoalescence of droplets, *Eur. J. Mech. B/Fluids*, Vol. 80, pp. 206–215, 2020.
- [5] Li, B., Vivacqua V., Wang J., Wang Z., Sun Z., Wang Z., Ghadiri M., Electrocoalescence of water droplets in sunflower oil using a novel electrode geometry, *Chem. Eng. Res. Des.*, Vol. 152, pp. 226–241, 2019.
- [6] Washizu M., Electrostatic actuation of liquid droplets for micro-reactor applications, *IEEE Trans. Ind. Applicat.*, Vol. 34 (4), pp. 732–737, 1998.
- [7] Gu H., Duits M.H.G., and Mugele F., Droplets formation and merging in two-phase flow microfluidics, *Int. J. Mol. Sci.*, Vol. 12 (4), pp. 2572–2597, 2011.
- [8] Tomar G., Gerlach D., Biswas G., Alleborn N., Sharma A., Durst F., Welch S.W.J., and Delgado A., Two-phase electrohydrodynamic simulations using a volume-of-fluid approach, *J. Comput. Phys.*, Vol. 227 (2), pp. 1267–1285, 2007.
- [9] López-Herrera J.M., Popinet S., and Herrada M.A., A charge-conservative approach for simulating electrohydrodynamic two-phase flows using volume-of-fluid, *J. Comput. Phys.*, Vol. 230 (5), pp. 1939–1955, 2011.
- [10] Tarantsev K.V., Modeling of the processes of coagulation and dispersion of water in low-conductive fluids in an electric field, *Surf. Eng. Appl. Electrochem.*, Vol. 49 (5), pp. 414–422, 2013.
- [11] Li, B., Wang, Z., Vivacqua, V., Ghadiri, M., Wang, J., Zhang, W., Wang, D., Liu, H., Sun, Z., Wang, Z., Drop-interface electrocoalescence mode transition under a direct current electric field, *Chem. Eng. Sci.*, Vol. 213, p. 115360, 2020.
- [12] Chirkov V.A., Gazaryan A.V., Kobranov K.I., Utiugov G.O., and Dobrovolskii I.A., A modification of the phase-field method to simulate electrohydrodynamic processes in two-phase immiscible liquids and its experimental verification, *J. Electrostat.*, Vol. 107, p. 103483, 2020.
- [13] Langer J.S., Models of pattern formation in first-order phase transitions, in *Directions in Condensed Matter Physics*, G. Grinstein and G. Mazenko, Eds. Singapore: World Scientific, pp. 165–186, 1986.
- [14] Osher S. and Sethian J.A., Fronts propagating with curvature-dependent speed: Algorithms based on Hamilton-Jacobi formulations, *J. Comput. Phys.*, Vol. 79 (1), pp. 12–49, 1988.
- [15] Yue P., Zhou C., Feng J.J., Ollivier-Gooch C.F., and Hu H.H., Phase-field simulations of interfacial dynamics in viscoelastic fluids using finite elements with adaptive meshing, *J. Comput. Phys.*, Vol. 219 (1), pp. 47–67, 2006.
- [16] Roy S., Anand V., and Thaokar R.M., Breakup and non-coalescence mechanism of aqueous droplets suspended in castor oil under electric field, *J. Fluid Mech.*, Vol. 878, pp. 820–833, 2019.
- [17] Huang X., He L., Luo X., Yin H., and Yang D., Deformation and coalescence of water droplets in viscous fluid under a direct current electric field, *Int. J. Multiph. Flow*, Vol. 118, pp. 1–9, 2019.
- [18] Sunder S. and Tomar G., Numerical investigation of a conducting drop’s interaction with a conducting liquid pool under an external electric field, *Eur. J. Mech. B/Fluids*, Vol. 81, pp. 114–123, 2020.
- [19] Sussman M. and Puckett E.G., A coupled level set and volume-of-fluid method for computing 3D and axisymmetric incompressible two-phase flows, *J. Comput. Phys.*, Vol. 162 (2), pp. 301–337, 2000.
- [20] Lin Y., Two-phase electro-hydrodynamic flow modeling by a conservative level set model, *Electrophoresis*, Vol. 34 (5), pp. 736–744, 2013.
- [21] Hirt C.W., Amsden A.A., and Cook J.L., An arbitrary Lagrangian-Eulerian computing method for all flow speeds, *J. Comput. Phys.*, Vol. 14 (3), pp. 227–253, 1974.

- [22] Xia Y. and Reboud J.L., Hydrodynamic and electrostatic interactions of water droplet pairs in oil and electrocoalescence, *Chem. Eng. Res. Des.*, Vol. 144, pp. 472–482, 2019.
- [23] Chirkov V.A., Reznikova M.P., Lashko A.V., and Dobrovolskii I.A., A Method to determine the interfacial tension for the conductive medium / liquid dielectric couple, *2018 IEEE 2nd International Conference on Dielectrics*, Budapest, Hungary, pp. 1–4, 2018.
- [24] Raisin J., Reboud J.-L., and Atten P., Electrically induced deformations of water–air and water–oil interfaces in relation with electrocoalescence, *J. Electrostat.*, Vol. 69 (4), pp. 275–283, 2011.
- [25] Chirkov V., Lashko A., and Reznikova M., The investigation of the Transition from Electrical Coalescence to Non-coalescence of Two Water Droplets, *2017 Annual Meeting of the Electrostatics Society of America*, Ottawa, Canada, pp. 1–8, 2018.
- [26] Anand V., Juvekar V.A., and Thaokar R.M., An experimental study on the effect of conductivity, frequency and droplets separation on the coalescence of two aqueous drops under an electric field, *Chem. Eng. Res. Des.*, Vol. 152, pp. 216–225, 2019.
- [27] Anand V., Juvekar V.A., and Thaokar R.M., Modes of coalescence of aqueous anchored drops in insulating oils under an electric field, *Colloids Surfaces A: Physicochem. Eng. Asp.*, Vol. 568, pp. 294–300, 2019.
- [28] Yang D., Ghadiri M., Sun Y., He L., Luo X., and Lü Y., Critical electric field strength for partial coalescence of droplets on oil–water interface under DC electric field, *Chem. Eng. Res. Des.*, Vol. 136, pp. 83–93, 2018.
- [29] Yeoh O.H., Some forms of the strain energy function for rubber, *Rubber Chem. Technol.*, Vol. 66, pp. 754–771, 1993.
- [30] Roy S. and Thaokar R. M., Numerical study of coalescence and non-coalescence of two conducting drops in a non-conducting medium under electric field, *J. Electrostat.*, Vol. 108 (September), p. 103515, 2020.
- [31] Chirkov V., Lashko A., Reznikova M., and Gazaryan A., Numerical and Experimental Investigation of Water Droplet Electrical Coalescence and Non-coalescence, *2018 Electrostatics Joint Conference, Boston, USA*, pp. 1–8, 2018.
- [32] Chirkov V. and Utiugov G., Features of quantitative verification of numerical models for computing electrohydrodynamic processes in two-phase immiscible liquids, *2020 IEEE Industry Applications Society Annual Meeting*, pp. 1–6, 2020.